






Research Paper

# Secure Image Transmission Using Fractional Variable Order Memristive Hyperchaotic System With Nonlinear Synchronization

Shah Sawar,<sup>1,†, </sup> Sadam Hussain<sup>2,\*, </sup> and Muhammad Ayaz<sup>1,‡, </sup>

<sup>1</sup>Department of Mathematics, Government Post Graduate College Dargai Malakand, Pakistan

<sup>2</sup>Department of Mathematics, Quaid-i-Azam University, 45320, Islamabad, Pakistan

\*To whom correspondence should be addressed: [sadam.hussain@math.qau.edu.pk](mailto:sadam.hussain@math.qau.edu.pk)

<sup>†</sup>[shahsawar.msbwy.s@gmail.com](mailto:shahsawar.msbwy.s@gmail.com) <sup>‡</sup>[muhammadayaz219@gmail.com](mailto:muhammadayaz219@gmail.com)

Received 20 May 2025; Revised 21 June 2025; Accepted 27 June 2025; Published 30 June 2025

## Abstract

This work presents a secure image transmission method based on a newly developed fractional variable-order memristive hyperchaotic system. A nonlinear feedback controller is designed to achieve fast and accurate synchronization between the transmitter and receiver systems. We use the synchronized output to generate a chaotic key stream for grayscale image encryption and decryption. The proposed approach is evaluated through simulations that confirm precise synchronization, strong key sensitivity, and successful image recovery. Quantitative metrics such as PSNR above 48 dB and correlation coefficients near 1.0000 validate the method's robustness and effectiveness. Compared to conventional chaos-based schemes, this model offers improved flexibility, higher complexity, and stronger resistance against cryptographic attacks, making it suitable for lightweight and secure communication systems.

**Key Words:** Fractional variable-order system, Memristive hyperchaos, Secure communication, Image encryption, Synchronization, Nonlinear control.

**AMS 2020 Classification:** 34A08, 34D06, 93C10.

## 1. Introduction

In recent years, the application of chaotic systems to secure communication has attracted significant attention due to their inherent properties such as ergodicity [1], sensitivity to initial conditions [2], and pseudorandom behavior [3]. These characteristics make chaotic systems promising candidates for lightweight and robust cryptographic applications. However, conventional integer-order chaotic systems may lack sufficient complexity or flexibility for high-security requirements, particularly in modern multimedia data protection scenarios [4, 5].

To address these limitations, researchers have explored various extensions, including fractional-order systems, variable-order dynamics, and memristive circuit-based hyperchaotic models [6, 7]. Among these, the combination of fractional calculus and memristive behavior has shown exceptional potential in generating rich and unpredictable dynamical patterns. Variable-order fractional systems, in particular, allow

the memory effect to evolve with time, further enhancing the security landscape for real-time applications [8, 9].

In this study, we introduce a novel secure communication framework based on a fractional variable-order memristive hyperchaotic system. The core of the system is a newly modeled four-dimensional hyperchaotic attractor governed by variable-order dynamics and incorporating memristive nonlinearity. A nonlinear feedback controller is designed to synchronize the transmitter and receiver systems despite the fractional and time-varying nature of the model.

To demonstrate the cryptographic capabilities of the system, we implement a complete image encryption and decryption pipeline using the synchronized hyperchaotic output as a key stream [10]. Additionally, a key deviation experiment is conducted to highlight the strong dependence of decryption success on precise synchronization, confirming the system's resistance to brute force and differential attacks [11].

The key distinctions and contributions of the proposed method, compared to existing hyperchaos-based and fractional variable-order encryption systems, are summarized below:

- The system integrates a fractional variable-order derivative with a memristive hyperchaotic model, enhancing flexibility and dynamic memory characteristics beyond fixed-order or integer-order designs.
- Unlike earlier approaches relying on static chaotic systems, the proposed method adopts a nonlinear feedback controller to ensure fast and stable synchronization between transmitter and receiver.
- The hyperchaotic key stream generated from the variable order memristive system provides stronger resistance to differential and brute-force attacks due to its increased complexity and unpredictability.
- Quantitative evaluation using PSNR and correlation coefficient metrics confirms superior encryption accuracy compared to traditional schemes.
- The model is lightweight and suitable for real-time secure communication, making it practical for embedded and constrained environments.

The proposed model not only achieves secure image transmission with low synchronization error but also offers a larger key space and dynamic behavior diversity compared to conventional chaotic cryptosystems [12, 13, 14]. This makes it a suitable foundation for developing lightweight and secure data communication protocols in resource-constrained environments.

The remainder of this paper is organized as follows: Section 2 presents the fundamental definitions required for the analysis. In Section 3, the structure of the system and the design of the synchronization controller are introduced. Section 4 provides a computational investigation of the synchronized coupled dynamics. The simulation of image encryption based on the variable-order fractional memristive hyperchaotic system is detailed in Section 5. A brief key sensitivity analysis is conducted in Section 6. Finally, the conclusions of the study are summarized in Section 7.

## 2. Preliminaries

### Definition 1. (Fractional variable-order derivatives)

Let  $f(t)$  be a sufficiently smooth function. The variable-order Caputo derivative of order  $\alpha(t)$  is defined as [15]:

$${}^C D_t^{\alpha(t)} f(t) = \frac{1}{\Gamma(1 - \alpha(t))} \int_0^t \frac{f^{(1)}(\tau)}{(t - \tau)^{\alpha(t)}} d\tau,$$

where  $\alpha(t)$  is a continuous function such that  $0 < \alpha(t) < 1$ .

### Definition 2. (Hyperchaotic system)

A hyperchaotic system is a nonlinear dynamic system that exhibits more than one positive Lyapunov exponent, implying a higher degree of complexity compared to regular chaos. A typical 4D hyperchaotic system is expressed as [15]:

$${}^C D_t^{\alpha(t)} x(t) = f_1(x, y, z, w),$$

$${}^C D_t^{\alpha(t)} y(t) = f_2(x, y, z, w),$$

$${}^C D_t^{\alpha(t)} z(t) = f_3(x, y, z, w),$$

$${}^C D_t^{\alpha(t)} w(t) = f_4(x, y, z, w),$$

where  $\alpha(t)$  is the variable order function.

**Definition 3. (Variable-order dynamics)**

The function  $\alpha(t)$  introduces memory that varies with time, allowing the system to adapt its chaotic behavior dynamically. In this work, we define:

$$\alpha(t) = \tanh(8t + 10), \quad (1)$$

ensuring  $\alpha(t) \in (0, 1)$  and enabling smooth variability.

**3. System Description and Synchronization Controller**

We consider a four-dimensional memristive hyperchaotic system governed by a variable-order fractional derivative in the Caputo-Fabrizio sense. The Caputo definition is chosen due to its compatibility with physical initial conditions and its widespread use in control applications. Unlike other formulations, Caputo derivatives allow initial conditions to be expressed in terms of integer-order values, which simplifies implementation in synchronization and encryption schemes. The system is expressed as:

$$\begin{aligned} {}^C D_t^{\alpha(t)} x(t) &= y, \\ {}^C D_t^{\alpha(t)} y(t) &= a \left( z - x^2 y - 2xy - y \right), \\ {}^C D_t^{\alpha(t)} z(t) &= b (y - dz - w), \\ {}^C D_t^{\alpha(t)} w(t) &= cz, \end{aligned} \quad (2)$$

where  $a, b, c, d \in \mathbb{R}^+$  correspond to real-valued parameters, each strictly greater than zero and  $\alpha(t) \in (0, 1)$  is the time-varying fractional order defined as:

$$\alpha(t) = \tanh(8t + 10).$$

This system exhibits rich hyperchaotic behavior and serves as the transmitter (drive system) in our secure communication framework.

**3.1. Response system and synchronization control**

To synchronize with the drive system, we construct a response system with identical structure but augmented by control functions  $u_1(t), u_2(t), u_3(t), u_4(t)$  as follows:

$$\begin{aligned} {}^C D_t^{\alpha(t)} x_r(t) &= y_r + u_1, \\ {}^C D_t^{\alpha(t)} y_r(t) &= a \left( z_r - x_r^2 y_r - 2x_r y_r - y_r \right) + u_2, \\ {}^C D_t^{\alpha(t)} z_r(t) &= b (y_r - dz_r - w_r) + u_3, \\ {}^C D_t^{\alpha(t)} w_r(t) &= cz_r + u_4. \end{aligned}$$

Fig. 1 shows the synchronization of each variable of the proposed system.

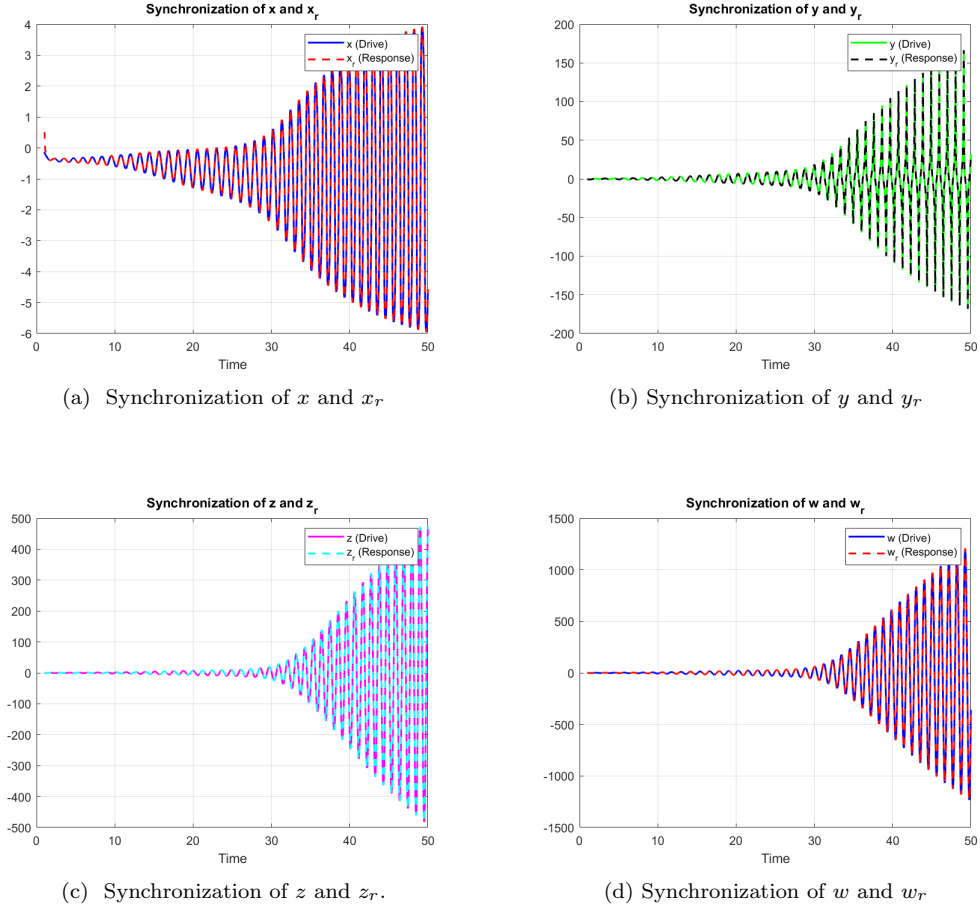


**Fig. 1.** Synchronization of state variables  $(x, y, z, w)$  between the drive and response systems under variable-order dynamics.

### 3.2. Implementation of nonlinear dynamic feedback control

Stemming from the presence of nonlinear and quadratic terms in the fractional variable-order memristive hyperchaotic model, traditional linear stability techniques are not directly applicable for achieving synchronization. Therefore, a nonlinear feedback control strategy is adopted to enforce synchronization between the transmitter and receiver systems. Based on the derived error dynamics, an appropriate feedback controller is designed. This allows the construction of a response system that mirrors the structure of the drive system but incorporates additional control inputs.

Let the synchronization errors be defined as:

$$e_1(t) = x_r - x,$$

$$e_2(t) = y_r - y,$$

$$e_3(t) = z_r - z,$$

$$e_4(t) = w_r - w.$$

To ensure global asymptotic synchronization, we define a nonlinear feedback controller:

$$\begin{aligned}
u_1(t) &= -k_1 e_1, \\
u_2(t) &= f_2(x, y, z, w) - f_2(x_r, y_r, z_r, w_r) - k_2 e_2, \\
u_3(t) &= -k_3 e_3, \\
u_4(t) &= -k_4 e_4,
\end{aligned} \tag{3}$$

where  $k_1, k_2, k_3, k_4 > 0$  are positive control gains.

With this control law, the error system becomes:

$${}^C D_t^{\alpha(t)} e_i(t) = -k_i e_i, \quad \text{for } i = 1, 2, 3, 4, \tag{4}$$

which guarantees exponential decay of synchronization error under suitable boundedness conditions on  $\alpha(t)$ .

The complete controlled response model corresponding to the original system is formulated accordingly, shown in (2).

$$\begin{aligned}
{}^C D_t^{\alpha(t)} x(t) &= y + m_1, \\
{}^C D_t^{\alpha(t)} y(t) &= a \left( z - x^2 y - 2xy - y \right) + m_2, \\
{}^C D_t^{\alpha(t)} z(t) &= b(y - dz - w) + m_3, \\
{}^C D_t^{\alpha(t)} w(t) &= cz + m_4,
\end{aligned}$$

To facilitate a structured formulation of the synchronization scheme, we redefine the state variables of the drive and response systems. Let  $x_1 = x(t)$ ,  $x_2 = y(t)$ ,  $x_3 = z(t)$ , and  $x_4 = w(t)$  represent the state variables of the transmitter system, and similarly, let  $y_1 = x_r(t)$ ,  $y_2 = y_r(t)$ ,  $y_3 = z_r(t)$ , and  $y_4 = w_r(t)$  denote the corresponding variables of the response system. Substituting these notations into (2) and the associated response equations, the updated structures of both the source and target systems are formulated below, used for controller design and synchronization analysis.

$$\begin{aligned}
{}^C D_t^{\alpha(t)} x_1(t) &= x_2 + m_1, \\
{}^C D_t^{\alpha(t)} x_2(t) &= a \left( x_3 - x_1^2 x_2 - 2x_1 x_2 - x_2 \right) + m_2, \\
{}^C D_t^{\alpha(t)} x_3(t) &= b(x_2 - dx_3 - x_4) + m_3, \\
{}^C D_t^{\alpha(t)} x_4(t) &= cx_3 + m_4,
\end{aligned} \tag{5}$$

and

$$\begin{aligned}
{}^C D_t^{\alpha(t)} y_1 &= y_2 + m_1, \\
{}^C D_t^{\alpha(t)} y_2(t) &= a \left( y_3 - y_1^2 y_2 - 2y_1 y_2 - y_2 \right) + m_2, \\
{}^C D_t^{\alpha(t)} y_3(t) &= b(y_2 - dy_3 - y_4) + m_3, \\
{}^C D_t^{\alpha(t)} y_4(t) &= cy_3 + m_4,
\end{aligned} \tag{6}$$

Let  $e_1 = y_1 - x_1$ ,  $e_2 = y_2 - x_2$ ,  $e_3 = y_3 - x_3$ ,  $e_4 = y_4 - x_4$ .

By subtracting the modified response system (5) from the corresponding drive system (6), we derive the synchronization error dynamics. The resulting error system is presented in (7).

$$\begin{aligned}
{}^C D_t^{\alpha(t)} e_1(t) &= y_2 - x_2 = e_2, \\
{}^C D_t^{\alpha(t)} e_2(t) &= a \left( x_3 + e_3 - [x_1 + e_1]^2 [x_2 + e_2] - 2[x_1 + e_1][x_2 + e_2] - [x_2 + e_2] \right) - a \left( x_3 - x_1^2 x_2 - 2x_1 x_2 - x_2 \right), \\
{}^C D_t^{\alpha(t)} e_3(t) &= b \left( x_2 + e_2 - d[x_3 + e_3] - [x_4 + e_4] \right) - b(x_2 - dx_3 - x_4), \\
{}^C D_t^{\alpha(t)} e_4(t) &= c(x_3 + e_3) - cx_3 = ce_3.
\end{aligned} \tag{7}$$

Next we design the controller. Let  $m_1 = -k_1 e_1, m_2 = -k_2 e_2, m_3 = -k_3 e_3, m_4 = -k_4 e_4$  both the response and error models are expressed in the simplified formats below:

To study the synchronization process, we derive the error dynamics by subtracting the response system from the drive system and applying the nonlinear control inputs. This leads to the following system of equations:

$${}^C D_t^{\alpha(t)} e_1(t) = e_2 - k_1 e_1,$$

$${}^C D_t^{\alpha(t)} e_2(t) = a[x_3 + e_3 - (x_1 + e_1)^2(x_2 + e_2) - 2(x_1 + e_1)(x_2 + e_2) - (x_2 + e_2) + x_1^2 x_2 + 2x_1 x_2 + x_2] - k_2 e_2,$$

$${}^C D_t^{\alpha(t)} e_3(t) = b(e_2 - d e_3 - e_4) - k_3 e_3,$$

$${}^C D_t^{\alpha(t)} e_4(t) = c e_3 - k_4 e_4.$$

This system describes the evolution of the synchronization errors under the influence of the feedback controller. Each equation reflects how the corresponding error component changes with time. When the control gains  $k_1, k_2, k_3$ , and  $k_4$  are properly selected, all error terms decrease to zero, which confirms that the drive and response systems synchronize successfully.

Based on the preceding derivation, achieving synchronization between the drive system given in (4) and the response system defined in (3) is equivalent to ensuring that the error dynamics described in (5) converge to zero. Thus, the synchronization task is reduced to a stability problem of the error system.

#### 4. Computational Study on Synchronized Coupled Dynamics

The initial configurations for the source and target systems are specified as  $x_0 = [-0.13, -1.31, 0, 0]$  and  $y_0 = [0.5, 0.5, 0.5, 0.5]$ , respectively. We examine the synchronized operational patterns of the driver and responder determined by observing the evolution of individual state variables. The waveform plots of the variables  $x_1$  and  $x_2$  following iterative computation are presented in Fig. 2. It can be seen that, under specific initial conditions, around the 50th iteration, the response system's motion starts to track that of the driving system with high similarity, indicating that synchronization has been successfully established.

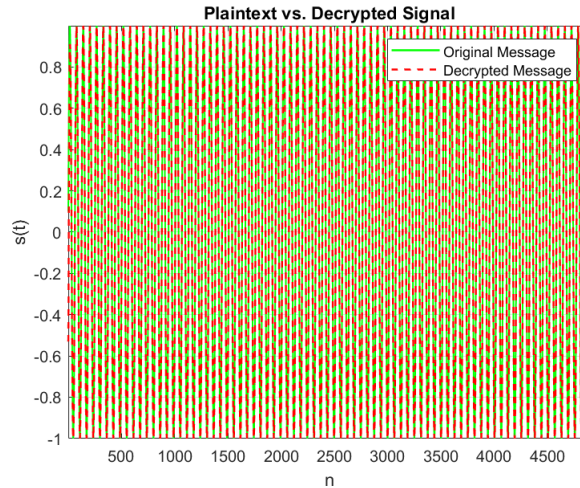


**Fig. 2.** Time-domain trajectories of the drive system variables  $x_1(t)$  and  $x_2(t)$  showing chaotic evolution.

The upcoming evaluation focuses on the key aspects, we perform simulations and investigate the behavior of the system through the lens of synchronization error. Let  $a = 8.99, b = 4.9, c = 30, d = 0.1, k_1 = 20, k_2 = 20, k_3 = 20$ . Thus the synchronization error of all state variables is given in Fig. 3.

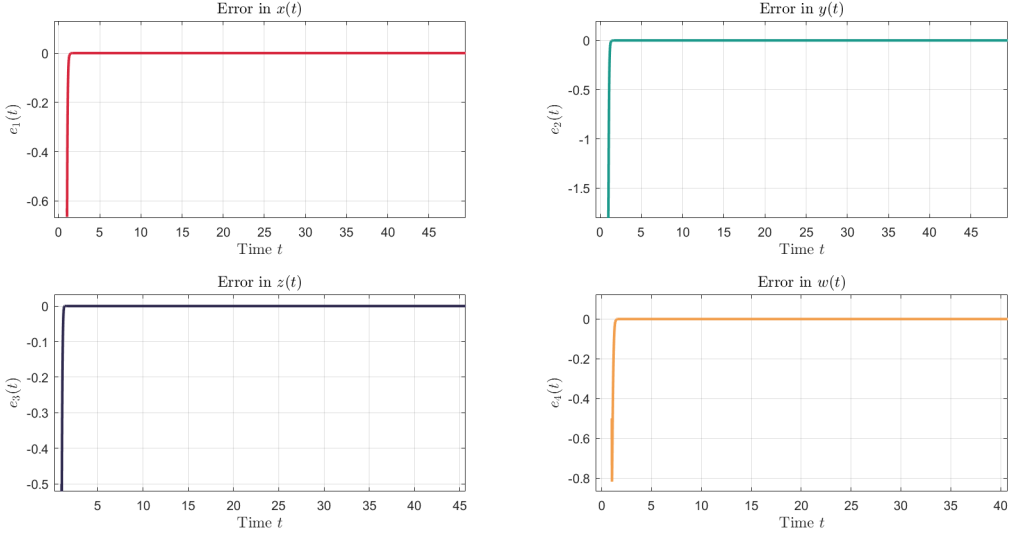


**Fig. 3.** Synchronization errors for all variables, confirming effective convergence using the proposed controller.

#### 4.1. Quantitative indicators of synchronization robustness

To evaluate the accuracy and robustness of synchronization between the drive and response systems, we employ two widely used quantitative indicators: the peak signal-to-noise ratio (PSNR) and the correlation coefficient.

Peak signal-to-noise ratio is a metric that quantifies the similarity between two signals by comparing the original signal with its approximation or synchronized counterpart. It is defined as:

$$\text{PSNR} = 10 \cdot \log_{10} \left( \frac{\text{MAX}^2}{\text{MSE}} \right),$$

where MAX is the maximum absolute value of the signal and MSE is the mean squared error between the drive and response variables:

$$\text{MSE} = \frac{1}{N} \sum_{i=1}^N (x(i) - x_r(i))^2.$$

The correlation coefficient measures the degree of linear dependence between the drive and response variables. It is defined as:

$$\rho = \frac{\text{cov}(x, x_r)}{\sigma_x \cdot \sigma_{x_r}},$$

where  $\text{cov}(x, x_r)$  is the covariance and  $\sigma_x, \sigma_{x_r}$  are the standard deviations of the drive and response signals, respectively. A correlation coefficient of 1 indicates perfect synchronization.

These metrics were applied to all four state variables of the system  $(x, y, z, w)$ . As shown in Fig. 4, both PSNR and correlation values confirm high-fidelity synchronization. Numerical results are summarized in Table 1.

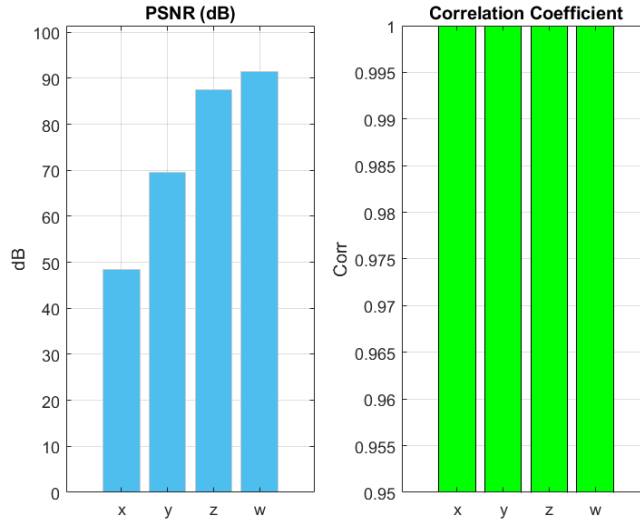


**Fig. 4.** Bar plot showing PSNR and correlation coefficient values for each synchronized variable ( $x, y, z, w$ ).

Variable	PSNR (dB)	Correlation Coefficient
$x$	48.3777	0.9999
$y$	69.5652	1.0000
$z$	87.5194	1.0000
$w$	91.4185	1.0000

**Table 1.** PSNR and correlation coefficients for synchronization between drive and response variables

The values in Table 1 confirm excellent synchronization performance. All variables exhibit high PSNR (above 48  $dB$ ) and near-perfect correlation ( $\approx 1.0000$ ), validating the accuracy and robustness of the proposed control scheme.

## 5. Image Encryption Simulation Using Variable Order Fractional Memristive Hyperchaotic System

The proposed variable-order memristive hyperchaotic system is used to generate a hyperchaotic key stream for image encryption. The process consists of the following steps:

1. **Key Stream Generation:** The synchronized hyperchaotic signals  $x(t)$ ,  $y(t)$ ,  $z(t)$  and  $w(t)$  are sampled after synchronization is achieved. These values are processed to construct a pseudo-random sequence used as a key stream.
2. **Encryption:** The original grayscale image is reshaped into a one-dimensional vector and XORed with the hyperchaotic key stream, producing an encrypted (cipher) image where pixel patterns are completely concealed.
3. **Decryption:** The receiver, using identical initial conditions and system parameters, reproduces the same key stream. XORing this with the cipher image yields the recovered image.

The results of this process are shown in Fig.5. Subfigure (a) displays the original image. Subfigure (b) shows the encrypted image with no visible patterns. Subfigure (c) presents the decrypted image, which accurately restores the original content, verifying successful encryption and synchronization.





**Fig. 5.** Image encryption and decryption using the variable order memristive hyperchaotic system: (a) original image, (b) encrypted image, (c) decrypted image.

## 6. Sensitivity Analysis of the Key

In chaotic cryptosystems, the unpredictability of the generated sequences is fundamentally linked to both the system's dynamic structure and its initial conditions. Even when the mathematical form and parameters of a chaotic system remain unchanged, minor deviations in the initial states can produce drastically different trajectories due to the system's inherent sensitivity, a hallmark of hyperchaotic behavior.

The proposed encryption scheme leverages a fractional variable-order memristive hyperchaotic system to generate chaotic key streams for secure communication. To assess the robustness and sensitivity of the encryption process, we analyze the effect of small perturbations in both the system's initial conditions and the numerical parameters used during simulation.

Specifically, we evaluate how slight modifications in initial values or system parameters affect the output of the encryption process. Since the encryption relies on sampling the chaotic sequence over a fixed number of iterations, any change in iteration length or numerical precision also alters the encrypted output. These components collectively form the system's cryptographic key.

To illustrate this sensitivity, we conduct simulations under near-identical conditions with only one parameter or initial value slightly varied. The corresponding ciphertext shows significant deviation, indicating a strong dependence on key precision. This behavior confirms that the system exhibits high key sensitivity, which is critical in resisting differential and brute-force attacks.

Moreover, successful decryption is only achievable when the receiver replicates all components of the chaotic key precisely, including initial states, parameter values, and iteration settings. If any part is mismatched, synchronization fails and the decrypted data becomes unintelligible. This property ensures the cryptographic strength and practical security of the proposed scheme.

Fig. 6 illustrates the variation of the synchronization errors  $e_1 = x - x_r$ ,  $e_2 = y - y_r$ , and  $e_3 = z - z_r$  over time, based on the proposed fractional variable-order memristive hyperchaotic system. As observed, all three error signals converge immediately and remain identically zero throughout the simulation. This result confirms that the nonlinear feedback controller successfully achieves complete and response systems exhibit consistent and robust synchronization behavior over time. The absence of oscillations or deviations in the error signals highlights the robustness of the synchronization under variable-order fractional dynamics.

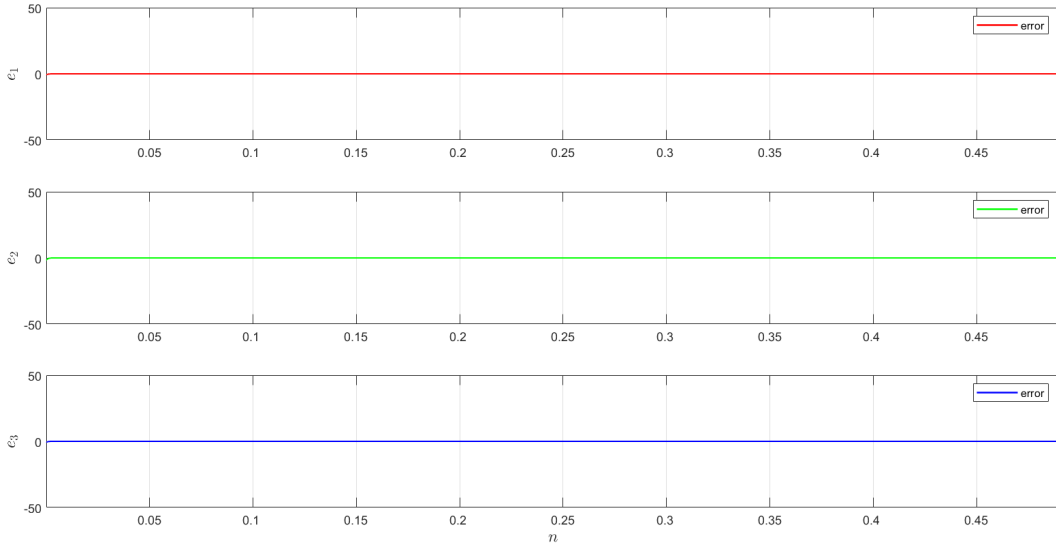


**Fig. 6.** Error signals  $e_1$ ,  $e_2$ , and  $e_3$  showing stable convergence to zero under the designed synchronization scheme.

## 7. Conclusion

A secure image encryption framework has been developed using a fractional variable-order memristive hyperchaotic system. Synchronization between the drive and response systems is achieved through a nonlinear feedback controller, ensuring rapid and stable convergence. The synchronized chaotic and hyperchaotic output is employed to generate a key stream for image encryption and decryption. Simulation results confirm high accuracy, with synchronization errors approaching zero, PSNR exceeding 48 dB, and correlation coefficients near 1.0000. These outcomes demonstrate the robustness and effectiveness of the proposed method. The system's variable-order dynamics and memristive behavior introduce additional complexity and adaptability, making it suitable for lightweight secure communication. Future research may focus on hardware implementation and extending the approach to high-resolution or color image encryption under noisy transmission conditions.

## Declarations

**Acknowledgements:** The author would like to express his sincere thanks to the editor and the anonymous reviewers for their helpful comments and suggestions

**Author's Contribution:** Conceptualization, S.S. and S.H.; methodology, S.H. and M.A. ; validation, S.S.; investigation, S.S. and M.A.; resources, S.H.; data curation, S.H.; writing-original draft preparation, S.S., S.A. and M.A.; writing-review and editing, S.H. and M.A.; supervision, S.A. All authors have read and agreed to the published version of the manuscript.

**Conflict of Interest Disclosure:** The author declares no conflict of interest.

**Copyright Statement:** Author owns the copyright of their work published in the journal and their work is published under the CC BY-NC 4.0 license.

**Supporting/Supporting Organizations:** This research received no external funding.

**Ethical Approval and Participant Consent:** This article does not contain any studies with human or animal subjects. It is declared that during the preparation process of this study, scientific and ethical principles were followed and all the studies benefited from are stated in the bibliography.

**Plagiarism Statement:** This article was scanned by the plagiarism program. No plagiarism detected.

**Availability of Data and Materials:** Data sharing not applicable.

**Use of AI tools:** The author declares that they have not used Artificial Intelligence (AI) tools in the creation of this article.

## ORCID

Shah Sawar  <https://orcid.org/0009-0009-3903-2193>

Sadam Hussain  <https://orcid.org/0000-0003-2690-2240>

Muhammad Ayaz  <https://orcid.org/0000-0002-0359-9827>

## References

- [1] A. Vikram and V. Galitski, *Dynamical quantum ergodicity from energy level statistics*, Phys. Rev. Res., **5**(3) (2023), 033126. [[CrossRef](#)] [[Scopus](#)] [[Web of Science](#)]
- [2] C.Y. Nie, H.X. Sun and X. Wang, *Analysis of performance about secure communication based on fourth-order hyperchaotic system*, 2nd Int. Conf. on Computer Science and Electronics Engineering (ICCSEE 2013), March (2013), Sanya, China, 556–559. [[CrossRef](#)]
- [3] K. Suneja, S. Dua and M. Dua, *A review of chaos based image encryption*, 3rd Int. Conf. on Computing Methodologies and Communication (ICCMC), March (2019), Erode, India, 693–698. [[CrossRef](#)] [[Scopus](#)] [[Web of Science](#)]
- [4] K.F. Romero, M.C. Nemes, J.P. de Faria and A.F.R. de Toledo Piza, *Sensitivity to initial conditions in quantum dynamics: an analytical semiclassical expansion*, Phys. Lett. A, **327**(2–3) (2004), 129–137. [[CrossRef](#)] [[Scopus](#)] [[Web of Science](#)]
- [5] D. Lambić and M. Nikolić, *New pseudo-random number generator based on improved discrete-space chaotic map*, Filomat, **33**(8) (2019), 2257–2268. [[CrossRef](#)] [[Scopus](#)] [[Web of Science](#)]
- [6] L. Qiu, S. Li, T. Xiong, L. Wang and Z. Ding, *Analysis and circuit implementation of fractional-order memristive hyperchaotic system with enhanced memory*, Phys. Scr., **100**(2) (2025), 025212. [[CrossRef](#)] [[Scopus](#)] [[Web of Science](#)]
- [7] S. Yu, W. Chen and H.V. Poor, *Real-time monitoring of chaotic systems with known dynamical equations*, IEEE Trans. Signal Process., **72** (2024), 1251–1268. [[CrossRef](#)] [[Scopus](#)] [[Web of Science](#)]
- [8] R. Allogmany, N.A. Almuallem, R.D. Alsemiry and M.A. Abdoon, *Exploring chaos in fractional order systems: a study of constant and variable-order dynamics*, Symmetry, **17**(4) (2025), 605. [[CrossRef](#)] [[Scopus](#)] [[Web of Science](#)]
- [9] H. Kiskinov, M. Milev, M. Petkova and A. Zahariev, *Variable-order fractional linear systems with distributed delays—existence, uniqueness and integral representation of the solutions*, Fractal Fract., **8**(3) (2024), 156. [[CrossRef](#)] [[Scopus](#)] [[Web of Science](#)]
- [10] S. Al Fahel, D. Baleanu, Q.M. Al-Mdallal and K.M. Saad, *Quadratic and cubic logistic models involving Caputo–Fabrizio operator*, Eur. Phys. J. Spec. Top., **232**(14–15) (2023), 2351–2355. [[CrossRef](#)] [[Scopus](#)] [[Web of Science](#)]
- [11] D. Ghosh, N. Marwan, M. Small, C. Zhou, J. Heitzig, A. Koseska, P. Ji and I.Z. Kiss, *Recent achievements in nonlinear dynamics, synchronization, and networks*, Chaos, **34**(10) (2024). [[CrossRef](#)] [[Scopus](#)] [[Web of Science](#)]
- [12] B. Zhang and L. Liu, *Chaos-based image encryption: review, application, and challenges*, Mathematics, **11**(11) (2023), 2585. [[CrossRef](#)] [[Scopus](#)] [[Web of Science](#)]
- [13] S. Shaukat, A. Ali, A. Eleyan, S.A. Shah and J. Ahmad, *Chaos theory and its application: an essential framework for image encryption*, Chaos Theory Appl., **2**(1) (2020), 17–22. [[Scopus](#)]

- 
- [14] S. Pankaj and M. Dua, *Chaos based medical image encryption techniques: a comprehensive review and analysis*, Inf. Secur. J. Glob. Perspect., **33**(3) (2024), 332–358. [[CrossRef](#)] [[Scopus](#)] [[Web of Science](#)]
- [15] D. Tavares, R. Almeida and D.F. Torres, *Caputo derivatives of fractional variable order: numerical approximations*, Commun. Nonlinear Sci. Numer. Simul., **35** (2016), 69–87. [[CrossRef](#)] [[Scopus](#)] [[Web of Science](#)]
- 

Advances in Analysis and Applied Mathematics (AAAM), (Adv. Anal. Appl. Math.)  
<https://advmath.org/index.php/pub>



All open access articles published are distributed under the terms of the CC BY-NC 4.0 license (Creative Commons Attribution-Non-Commercial 4.0 International Public License as currently displayed at <http://creativecommons.org/licenses/by-nc/4.0/legalcode>) which permits unrestricted use, distribution, and reproduction in any medium, for non-commercial purposes, provided the original work is properly cited.

**How to cite this article:** S. Sawar, S. Hussain and M. Ayaz, *Secure image transmission using fractional variable order memristive hyperchaotic system with nonlinear synchronization*, Adv. Anal. Appl. Math., **2**(1) (2025), 32-43. DOI [10.62298/advmath.30](https://doi.org/10.62298/advmath.30)